Virtual reality modelling based on computed tomography and three-dimensional angiography for planning of percutaneous and hybrid treatment in infants with pulmonary vein stenosis

Judyta Szeliga[1], Małgorzata Waśko[1], Jacek Kołcz[2], Andrzej Rudziński[1], Ryan Callahan[3], Sebastian Góreczny[1]

[1]Department of Pediatric Cardiology, University Children's Hospital, Faculty of Medicine, Jagiellonian University Medical College, Krakow, Poland

[2]Department of Paediatric Cardiac Surgery, University Children's Hospital, Jagiellonian University Medical College, Krakow, Poland

[3]Division of Cardiology, The Children's Hospital of Philadelphia and Department of Pediatrics, Perelman School of Medicine at the University of Pennsylvania, Philadelphia, PA, United States

Adv Interv Cardiol 2025; 21, 1 (79): 108–113
DOI: https://doi.org/10.5114/aic.2025.147992

Introduction

Paediatric pulmonary vein stenosis (PVS) is a rare, heterogeneous disease associated with significant morbidity and mortality [1]. Once considered lethal, it is now viewed as a chronic disease with improving survival rates [2]. PVS is characterized by progressive neointimal obstruction of the pulmonary veins, leading to secondary pulmonary hypertension (PH) and congestive heart failure (CHF). The paediatric spectrum includes primary and secondary PVS, further stratified by patient heterogeneity such as prematurity, genetic predisposition, congenital heart defects (especially abnormal pulmonary venous return) or previous surgical interventions [1, 3]. Current treatments focus on maintaining pulmonary vein patency through interdisciplinary efforts [1–3].

Trans-catheter interventions are widely accepted as the primary approach and have complex, personalized decision-making involved in the cases. Diverse techniques and equipment are used, including low- to high-pressure balloon catheters, cutting or drug-eluting balloons, and vascular stent implantation with drug-eluting stents outperforming bare-metal stents [4, 5].

Surgical treatment is foundational in cases of congenital heart defects, including isolated anomalous pulmonary venous return. In normally connected veins, surgery is predominantly utilized for anatomic specific lesions not amenable to percutaneous interventions or in some experienced centres, as primary therapy [3, 6].

Additionally, antiproliferative drugs such as imatinib, bevacizumab, and sirolimus are utilized by leading PVS centres to slow disease progression [1, 7]. Therapeutic success relies on early diagnosis and a multidisciplinary approach [1, 3].

Echocardiography serves as the primary tool for screening, diagnosis, tracking disease progression, and assessing treatment outcomes [1, 8]. Cardiac catheterization with hemodynamic and angiographic assessment remains the gold standard for detailed anatomical evaluation and PVS confirmation. Other comprehensive diagnostics using a broad range of imaging and functional studies are also utilized and include chest X-rays, computed tomography (CT) angiography, magnetic resonance imaging (MRI), radionuclide perfusion lung scanning, intravascular imaging, and rotational 3D angiography (3DRA) [1, 3, 9, 10]. Multimodal diagnostics enable successful diagnostic-therapeutic procedures.

We present our experience using VR models constructed from pre-procedural CT and 3DRA as a valuable supplement to standard imaging tools in planning and conducting procedures in 2 patients with congenital heart defects and PVS.

Corresponding author:
Sebastian Góreczny, Department of Pediatric Cardiology, University Children's Hospital, Faculty of Medicine, Jagiellonian University Medical College, Krakow, Poland, e-mail: sebastian.goreczny@uj.edu.pl
Received: 15.10.2024, **accepted:** 22.12.2024, **online publication:** 28.02.2025.

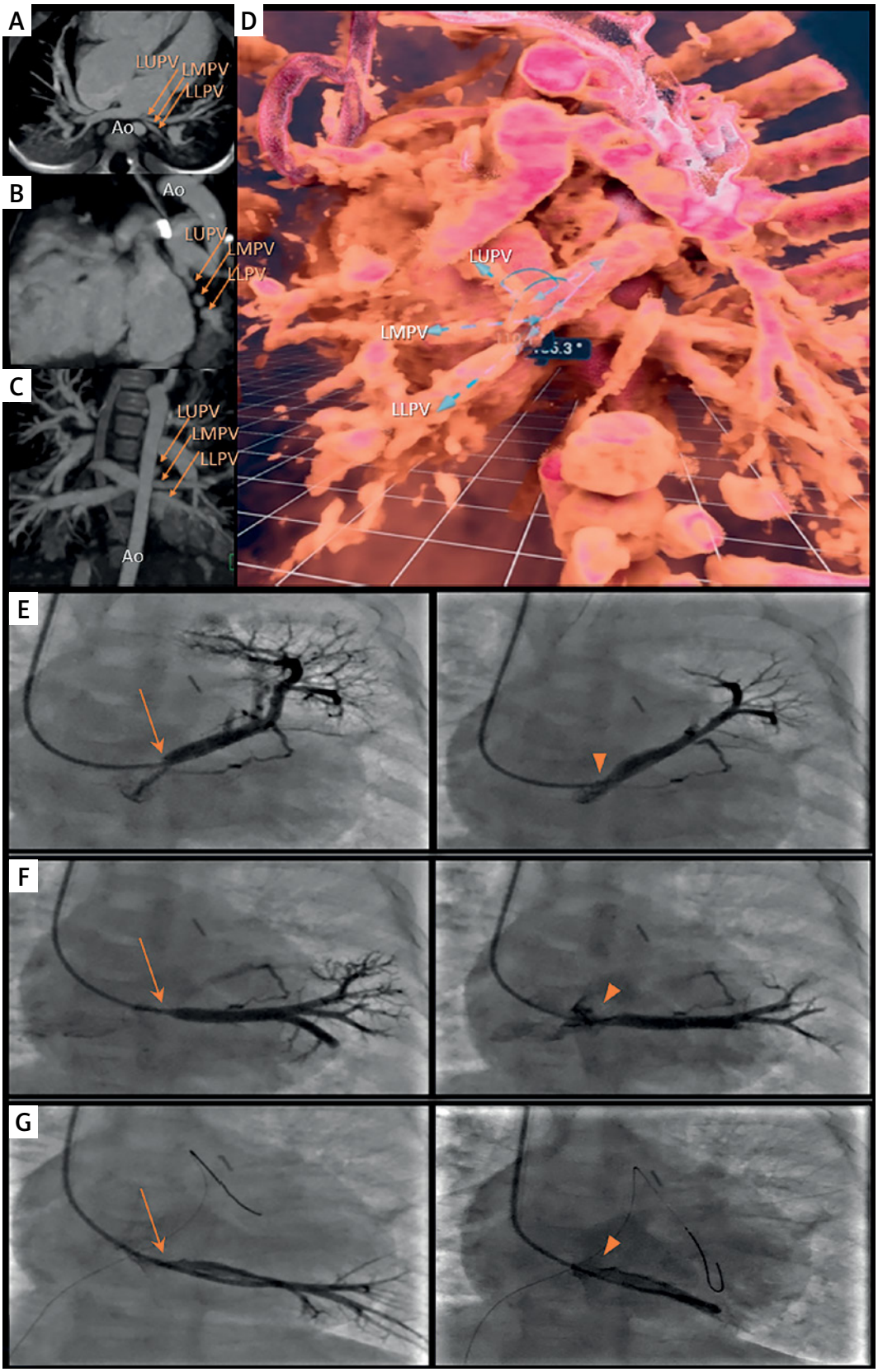

Figure 1. Multimodal imaging (CT, VR, 2D angiography) in the diagnostic and therapeutic process of patient 1. **A** – Axial view, **B** – sagittal view, **C** – coronal view of the CT scan. Arrows indicate the left upper pulmonary vein (LUPV), left middle pulmonary vein (LMPV), and left lower pulmonary vein (LLPV), respectively.

(Cont'd on next page)

The course of the vessels is shown in close proximity to the aorta (Ao). **D** – Virtual reality reconstruction, posterior view. The three narrowed left-sided pulmonary veins (upper – LUPV, middle – LMPV, and lower – LLPV) are shown from the back. Blue dashed arrows indicate the course and spatial arrangement of the vessels. **E** – Left image: Initial angiography, contrast injection into the left upper pulmonary vein (LUPV). Significant stenosis is visible, indicated by an orange arrow. Right image: Final angiography post-interventional procedure. The dilated stenotic segment is visible, indicated by an orange arrowhead. **F** – Left image: Initial angiography, contrast injection into the left middle pulmonary vein (LMPV). Significant stenosis is visible, indicated by an orange arrow. Right image: Final angiography post-interventional procedure. The dilated stenotic segment is visible, indicated by an orange arrowhead. **G** – Left image: Initial angiography, contrast injection into the left lower pulmonary vein (LLPV). Significant stenosis is visible, indicated by an orange arrow. Right image: Final angiography post-interventional procedure. The dilated stenotic segment is visible, indicated by an orange arrowhead

Case reports

Patient 1

The patient was born at 37 weeks of gestation, weighing 1980 g, with a complex congenital heart defect involving heterotaxy syndrome with right atrial isomerism, D-loop ventricles, double-outlet right ventricle (DORV), malposition of the arterial trunks, subvalvular pulmonary stenosis, and total anomalous pulmonary venous return (TAPVR) draining into the superior vena cava (SVC).

The surgical correction at 2 months of age aimed to address the TAPVR by connecting the pulmonary venous collector to the left atrium, reducing the atrial septal defect, and ligating the pulmonary venous collector at the junction with the SVC. However, due to hypotension, desaturation and circulatory failure in the immediate postoperative period, a partial reversal of the correction was performed by removing the interatrial septum patch and restoring communication between the pulmonary venous collector and the SVC while maintaining the pulmonary venous connection to the left atrium.

At 4 months of age (4.5 kg), echocardiographic examination revealed stenosis of the left pulmonary veins (LPVs) with a 5 mmHg mean gradient. CT confirmed stenosis of all 3 LPVs. Prompt cardiac catheterization via the inferior vena cava (IVC) allowed for effective balloon angioplasty of the left upper pulmonary vein (LUPV) (Ryujin 4 × 15 mm, Terumo and NC Emerge 5 × 15 mm, Boston) and left lower pulmonary vein (LLPV) (NC Emerge 6 × 15 mm), reducing mean gradients from 6 mm Hg to 3 mm Hg in the LUPV and from 8 mm Hg to 2 mm Hg in the LLPV, stabilizing the child's condition for the following 3 months.

At 7 months of age (5.4 kg), LPV re-stenosis was noted by echocardiography with a mean gradient of 5 mm Hg. Repeat CT showed re-stenosis of the 3 LPVs, located in close proximity to the aorta (Figures 1 A–C). The CT-based VR model (Vmersive, VR-learning, Poland; Figure 1 D) allowed precise spatial planning of the catheterization, including access from the SVC. All 3 stenosed LPV were successfully identified, and effective angioplasty was performed using a combination of balloon catheters with diameters of 4, 5, and 6 mm (Ryujin, NC Emerge), with reduction of mean gradients from 11 mm Hg to 1 mm Hg, measured in the LUPV and middle LPV (Figures 1 E–G). The follow-up echocardiogram demonstrated trivial LPV flow turbulence with a 2 mm Hg mean gradient.

Subsequently, the child was initiated on imatinib therapy following bioethics approval. Preliminary 5-month observations of pharmacotherapy are promising.

Patient 2

The patient was born at term (3.3 kg) with infracardiac TAPVR and underwent corrective surgery in the neonatal period, connecting the common pulmonary venous collector to the left atrium (LA) with partial atrial septal closure.

At 2 months of age (4 kg), echocardiography demonstrated stenosis at the collector-LA anastomosis with a mean gradient of 8 mm Hg, and the patient was referred for catheterization. The child underwent percutaneous intervention with 6 × 20 mm (NC Emerge) and 8 × 20 mm (Tyshak, NuMed) balloon angioplasty, reducing the mean gradient from 14 to 6 mm Hg.

One month later, echocardiography showed significant restenosis of the anastomosis, with the mean gradient increasing to 18 mm Hg. As a result, re-operation was performed to widen the stenosed venous collector using a matrix patch (ProxiCor, Aziyo Biologics, Inc).

Immediately after the operation, the mean echo gradient was 2 mm Hg. Two months afterwards (4.9 kg), following a sudden deterioration in the child's condition, echocardiography revealed a wide LA-collector junction with severe bilateral narrowing and turbulent flow with a 10 mm Hg and 24 mm Hg mean gradient from the left and right PVs, respectively. Additionally, echocardiography provided suspicion for spontaneous closure of the previously described inter-atrial communication, which was confirmed during subsequent cardiac catheterization.

Haemodynamics demonstrated elevated mean right and left wedge pressures of 16 mm Hg and 13 mm Hg, respectively. Detailed angiography evaluation (Figures 2 A–E), supplemented by 3DRA, confirmed proximal stenoses of all pulmonary veins.

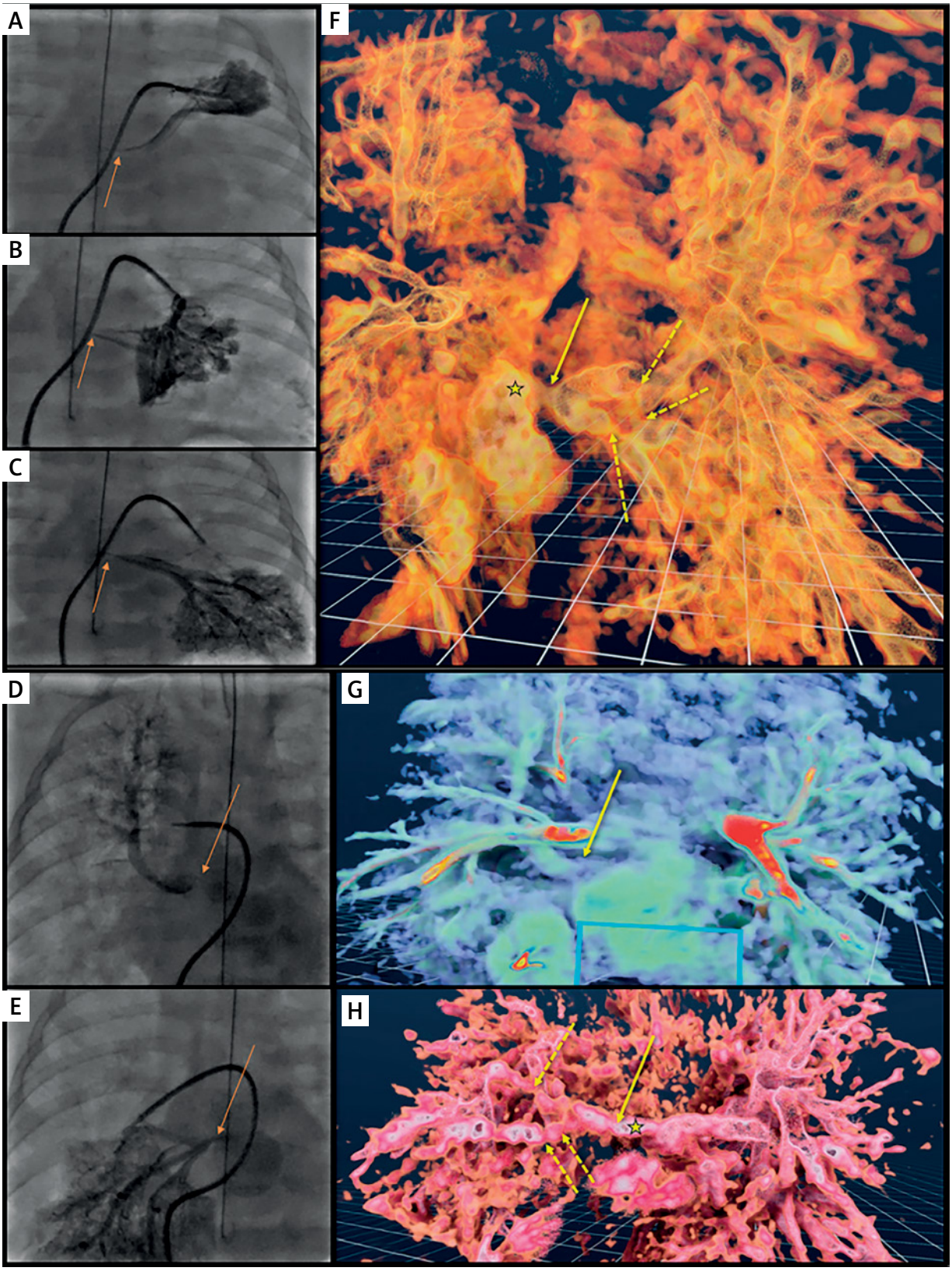

Figure 2. Multimodal imaging (2D angiography, 3D rotational angiography (3DRA) and virtual reality (VR) reconstruction) in the diagnostic process of patient 2. **A–C** – Initial angiography, selective wedge injections into the peripheral branches of the left pulmonary artery. The venous return is visualized in levophase.

(Cont'd on next page)

The site of stenosis is indicated by an orange arrow. **D** – Initial angiography, selective wedge injection into the lower lobe branch of the right pulmonary artery (RPA). The venous return is visualized in levophase. The site of stenosis is indicated by an orange arrow. **E** – Initial angiography, selective wedge injection into the upper lobe branch of the RPA. The venous return is visualized in levophase. The site of stenosis is indicated by an orange arrow. **F** – VR model reconstructed from 3DRA: the pulmonary veins draining the left lung converge and empty into a common vessel, which is significantly stenosed (yellow arrow) near its junction with the collector. Additional multi-level peripheral stenoses are visible (dashed yellow arrows). The 3DRA model corresponds to the angiograms in Figure 2 **A**–**C**. **G** – VR-3DRA reconstruction: model focused on the right upper pulmonary vein (RUPV). Significant stenosis of the RUPV entrance into the collector is indicated by a yellow arrow. The model aligns with Figure 2 **D**. **H** – VR-3DRA reconstruction: model focused on the right lower pulmonary vein (RLPV). Significant stenosis of the RLPV entrance into the collector is indicated by a yellow arrow. Additional multi-level peripheral stenoses are visible (dashed yellow arrows). The venous collector is marked with a yellow star. The model aligns with Figure 2 **E**

The assessment using 3DRA (2 ml/kg of 2 : 1 diluted contrast, 2 s delay, apnoea) in virtual reality software (Vmersive, Figures 2 F–H), allowed for a spatial relationships analysis and precise localization of the stenoses at the pulmonary vein openings to the collector on both sides. Additionally, the 3DRA-VR analysis, based on tissue density and utilizing tools from the software library, suggested the presence of peripheral pulmonary vein lesions (Figures 2 F, H). Based on this multimodality imaging, the child was scheduled for a hybrid procedure specifically tailored to their anatomy. The stenotic sites observed in 3DRA VR were confirmed intraoperatively, with significant neointimal hyperplasia as described. The combination of "sutureless" surgical technique on the right sided veins and intraoperative balloon angioplasty (PowerFlex 6 and 8 mm, Cordis) of the left sided veins resulted in a good post-operative outcome. Follow-up echocardiogram revealed a wide venous collector and residual trivial 3 mmHg mean gradient in the PVs. After the child's condition stabilised, they were initiated on imatinib therapy following bioethics approval. The current observation period for pharmacotherapy is 2 months.

Discussion

The presented cases demonstrate that effective VR models can be generated from both preprocedural CT and intraprocedural 3DRA. Moreover, these models allow for immersive spatial analysis, offering a significant advantage over traditional 2D screen-based 3D models. Our laboratory experience indicates that procedure planning based on CT and VR models is feasible for a wide range of patient ages and sizes [11, 12].

In the first patient, the VR-model immersive spatial assessment clearly demonstrated the problematic positioning of the left PVs between the atrium and the descending aorta. This analysis also enabled precise evaluation of complex vascular relationships involved, ostia locations and delineation of upstream anatomy. The imaging assisted in case planning, including utilizing the SVC, which improved catheter manoeuvrability and balloon support, leading to a shorter, more effective catheterization.

In the second case, 3DRA proved valuable for spatial defects analysis as a complementary method to standard 2D angiography. It yielded an immediate analysis that was sufficient for intra-procedural decision-making and future surgical planning and ultimately replaced the need for additional preoperative CT. The accuracy of the imaging was confirmed by direct visualisation during surgery and assisted the team in efficient localisation of the lesions.

Addressing complex issues such as pulmonary vein stenosis in paediatric patients requires excellent operator expertise in 3DRA [13], including precise contrast dosage, appropriate delay planning and apnoea, though not rapid pacing.

Pre-procedural planning of hybrid procedures based on VR reconstructions and simulations is an effective method successfully implemented at our institution, applicable to complex cases such as stent implantation in a severely narrowed pulmonary artery at risk of bronchial compression and in intricate aortic arch anatomies [14, 15].

Conclusions

In 2 patients with severe multivessel PVS, CT and 3DRA-generated VR models proved valuable for procedural planning, enhancing the precision and effectiveness of percutaneous and hybrid treatment. Further research into the role of imaging and virtual tools in complex cardiac defects is needed.

Acknowledgments

We are grateful to Aleksandra Dziewulska, Natalia Nawara-Węgrzyn and Maksym Lazu for excellent echocardiographic guidance.

Funding

The Virtual Reality project is supported by the Jagiellonian University Medical College internal grant No. N41/DBS/001219.

Ethical approval

Not applicable.

Conflict of interest

The authors declare no conflict of interest.

References

1. Callahan R, Morray BH, Hirsch R, et al. Management of pediatric pulmonary vein stenosis. J Soc Cardiovasc Angiogr Interv 2022; 1: 100391.
2. McLennan DI, Solano ECR, Handler SS, et al. Pulmonary vein stenosis: moving from past pessimism to future optimism. Front Pediatr 2021; 9: 747812.
3. Vanderlaan RD, Rome J, Hirsch R, et al. Pulmonary vein stenosis: treatment and challenges. J Thorac Cardiovasc Surg 2021; 161: 2169-76.
4. Kurita Y, Baba K, Kondo M, et al. Clinical outcomes after the endovascular treatments of pulmonary vein stenosis in patients with congenital heart disease. Cardiol Young 2019; 29: 1057-65.
5. Khan A, Qureshi AM, Justino H. Comparison of drug eluting versus bare metal stents for pulmonary vein stenosis in childhood. Catheter Cardiovasc Interv 2019; 94: 233-42.
6. Feins EN, Ireland C, Gauvreau K, et al. Pulmonary vein stenosis: anatomic considerations, surgical management, and outcomes. J Thorac Cardiovasc Surg 2022; 163: 2198-207.e3.
7. Callahan R, Esch JJ, Wang G, et al. Systemic sirolimus to prevent in-stent stenosis in pediatric pulmonary vein stenosis. Pediatr Cardiol 2020; 41: 282-9.
8. Callahan R, Gauthier Z, Toba S, et al. Correlation of intravascular ultrasound with histology in pediatric pulmonary vein stenosis. Children 2021; 8: 193.
9. Lee EY, Jenkins KJ, Vargas SO, et al. Thoracic multidetector computed tomography angiography of primary pulmonary vein stenosis in children: evaluation of characteristic extravascular findings. J Thorac Imaging 2021; 36: 318-25.
10. Roman KS, Kellenberger CJ, Farooq S, et al. Comparative imaging of differential pulmonary blood flow in patients with congenital heart disease: magnetic resonance imaging versus lung perfusion scintigraphy. Pediatr Radiol 2005; 35: 295-301.
11. Dziewulska A, Szeliga J, Góreczny S. Virtual reality modelling for planning of percutaneous first step palliation in a newborn with heterotaxy syndrome. Cardiol Young 2024; 34: 1612-4.
12. Góreczny S, Szeliga J, Lazu M, et al. First Polish pediatric experience with percutaneous self-expandable pulmonary valve implantation. Kardiol Pol 2024; 82: 101-2.
13. Szeliga J, Kołcz J, Piwowarczyk B, et al. Multimodality imaging and hybrid treatment of pulmonary artery stenosis in a patient with high risk of airway compression. Kardiol Pol 2023; 81: 1151-2.
14. Szeliga J, Lazu M, Góreczny S. Virtual reality modelling in a child after multiple interventions for hypoplastic aortic arch and coarctation. Cardiol Young 2024; 34: 1594-6.
15. Goreczny S, Moszura T, Lukaszewski M, et al. Three-dimensional image fusion of precatheter CT and MRI facilitates stent implantation in congenital heart defects. Rev Esp Cardiol 2019; 72: 512-4.